THE JOURNAL OF PHYSICAL CHEMISTRY C

Article

pubs.acs.org/JPCC

Hydrogen Adsorption on Small Zeolite-Supported Rhodium Clusters. A Density Functional Study

Velina K. Markova,[†] Georgi N. Vayssilov,[†] and Notker Rösch*[,‡,§]

[†]Faculty of Chemistry and Pharmacy, University of Sofia, Blvd. J. Baucher 1, 1126 Sofia, Bulgaria

[‡]Institute of High Performance Computing, Agency for Science, Technology and Research, 1 Fusionopolis Way, #16-16 Connexis, Singapore 138632, Singapore

[§]Department Chemie and Catalysis Research Center, Technische Universität München, 85747 Garching, Germany

Supporting Information

ABSTRACT: Using a periodic density functional approach, we modeled the dissociative adsorption of hydrogen on small Rh clusters, supported inside the cavity of a faujasite-type zeolite. H spillover from a zeolite hydroxyl group to the metal cluster is favorable by at least 160 kJ/mol. Therefore, we used the complexes HRh_3 and HRh_4 in deprotonated zeolite as reference for H adsorption from the gas phase. For the most stable location of the complexes, at three four-membered rings, the average adsorption interaction of hydrogen decreases monotonously with increasing H loading. Adsorption energies are calculated from −70 to −52 kJ/mol for the complexes H_3Rh_3 and H_7Rh_3, respectively, and from −67 to −47 kJ/mol for the complexes H_3Rh_4 and H_9Rh_4, respectively. The preferred coordination of H ligands changes with the H loading, bridging at Rh−Rh bonds at low loading and terminal at Rh centers at high loading. Concomitantly the average Rh−Rh nearest-neighbor distances increase from 242 to 272 pm (Rh_3) and from 247 to 265 pm (Rh_4). A thermodynamic model based on the calculated Gibbs free energies of the structures studied suggests that complexes with maximum H loading, H_7Rh_3 and H_9Rh_4, dominate in a wide range of H_2 pressures and temperature. The calculated atomic charges suggest that the metal moieties are oxidized due to reverse hydrogen spillover and adsorption of hydrogen from the gas phase.

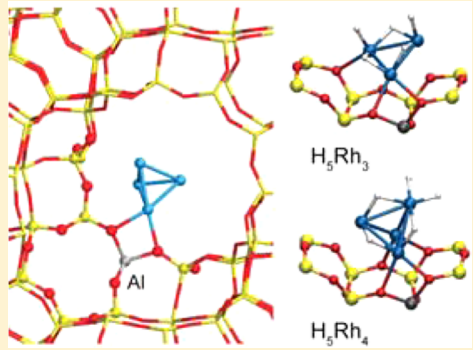

1. INTRODUCTION

Rhodium is known as one of the most active catalysts in various hydrogenation and dehydrogenation reactions.[1−23] The catalytic activity and selectivity of rhodium depends strongly on the nuclearity of the rhodium species. Recent studies of Gates et al.[4] showed that Rh complexes, supported on HY zeolite, catalyze the dimerization of ethene in the presence of H_2. However, when these complexes are transformed to small Rh clusters in zeolite cavities, the preferred selectivity changes to the hydrogenation of the C=C bond. The support plays a key role in stabilizing these small Rh complexes and clusters. In particular, in zeolites the preparation of supported small metal clusters is assisted by the well-defined chemical composition and the known size of the pores of these materials.[5−7] The size of the clusters was examined by EXAFS measurements; the coordination number of Rh was determined to be ∼1.9, corresponding to Rh_3 species.[4] Moreover, Gates et al. proposed[4] that dissociative adsorption of hydrogen from the gas phase takes place on the Rh clusters. Activation of the H−H bond on such small clusters may be one of the reasons why hydrogenation becomes the dominant reaction. Experimental studies of hydrogen adsorption on Rh, Ir, and Pt particles, supported on alumina or silica, revealed large amounts of hydrogen adsorbed on these metal species.[8] For Rh particles, the metal-to-hydrogen ratio M/H was determined at 1.98, close to the value of 2.25, determined in earlier density functional calculations on supported Rh_4 clusters.[9]

Hydrogen adsorption on metal clusters is an important step in a variety of important processes, e.g., the hydrogenation of olefins, hydrogen storage, and spillover. In this connection, it is important to study the structure, the relative stability, and the electronic properties of hydrogenated metal clusters as well as the effect of the support on the properties of these metal species. In previous density functional studies,[10] we modeled bare and hydrogenated metal clusters in zeolites, using zeolite fragments, either isolated[9,11,12] or embedded in a zeolite framework, represented by a force field.[13,14] In the present work, we report density functional calculations on the dissociative adsorption of hydrogen on small Rh_n clusters (n = 3, 4), supported inside the cavity of a faujasite-type zeolite framework. In the models, we applied periodic boundary conditions to describe the support as an ideal zeolite framework. With these model calculations we provide insight on the structure, the electronic properties, and the vibrational normal modes of small hydrogenated Rh clusters and how these properties change with H loading as well as with the size

Received: October 29, 2014
Revised: December 13, 2014
Published: December 30, 2014

DOI: 10.1021/jp510842q
J. Phys. Chem. C 2015, 119, 1121−1129

and the location of the clusters. We also constructed a thermodynamic model to predict how the hydrogen coverage of the metal clusters changes with temperature and hydrogen pressure.

2. COMPUTATIONAL DETAILS

2.1. Zeolite Models. All calculations were carried out using a faujasite-type zeolite framework, represented by a rhombic unit cell with the parameters $a = b = c = 17.34$ Å and $\alpha = \beta = \gamma = 60°$ (Figure S1 in Supporting Information, SI).[15,16] The unit cell comprises 48 T atoms, of which one is an Al atom, and the others are Si atoms. The negative charge of the framework was compensated by one bridging OH group, located at a four-membered ring close to the Al center. In the initial structure the OH group is located at an O1 site (Figure S2 of SI). Other positions of the OH group have not been modeled because the energy difference between different isomers[17,18] is 1 order of magnitude smaller than the energy of reverse hydrogen spillover (transfer of hydrogen from a hydroxyl group of the zeolite to the metal cluster).[10] Therefore, the initial position of the OH group may have a negligible influence on the energy of hydrogen transfer. We explored two adsorption sites for the Rh_n (n = 3, 4) clusters in the supercage of faujasite, near a six-membered (6R) and near three four-membered (4R) rings of the zeolite framework (Figure 1); for the location of the rings and the Al center, see Figure S1 of the SI.

We denote the structures with bare Rh clusters in the zeolite as Rh_3/ZOH and Rh_4/ZOH, whereas the structures formed after reverse hydrogen spillover from the zeolite hydroxyl group to the metal cluster are denoted as HRh_3/ZO and HRh_4/ZO.

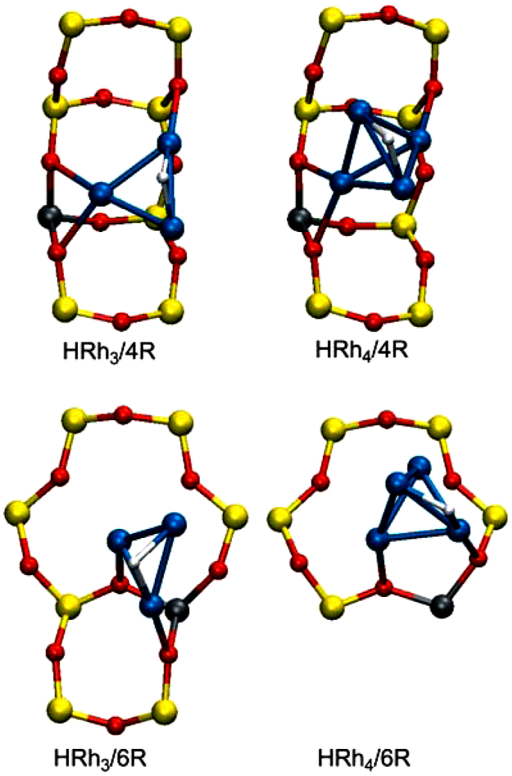

Figure 1. Coordination of HRh_n/ZO complexes near 4R sites of three four-membered rings (upper row) and six-membered ring (6R) sites (lower row). Color coding: Rh, blue; H, white; O, red; Si, yellow; Al, gray.

Because the latter type of species was calculated to be energetically favorable, we simulated the dissociative adsorption of up to four H_2 molecules on the tetrahedral cluster Rh_4 and up to three H_2 molecules on the cluster Rh_3. We shall denote these hydrogenated species as H_mRh_3/ZO (m = 1, 3 5, 7) and H_mRh_4/ZO (m = 1, 3, 5, 7, 9), respectively. The geometry optimizations were started from structures by adding two atomic H ligands to (relatively) free sites of the previously optimized metal moieties with two H ligands less. We tried at least two initial structures for each hydrogen coverage. Two coordination types were considered for the H ligands, terminal and bridging (2-fold).

2.2. Electronic Structure Method. For the periodic density functional calculations, we used the Vienna ab initio simulation package (VASP),[19,20] applying an exchange-correlation functional in the form of the generalized gradient approximation, specifically the functional suggested by Perdew, Burke, and Ernzerhof (PBE).[21] Given the large unit cell, we sampled the Brillouin zone at the Γ point only. We represented the ion−electron interactions with the projector augmented wave method (PAW).[22,23] The plane-wave representation of the valence wave functions was characterized by a cutoff energy of 400 eV. Self-consistency was considered to be reached when the total energy changed less than 10^{-6} eV between subsequent cycles; the geometry optimization was stopped when the force on each ion was less than 0.02 eV/Å. The relative stability and optimized structural parameters of all modeled isomeric structures are given in the SI: in Tables S1−S4 for the complexes Rh_3/ZOH and H_mRh_3/ZO and in Tables S5−S8 for the complexes Rh_4/ZOH and H_mRh_4/ZO. All optimized structures are shown in Figures S2−S6 of the SI.

To confirm that the geometry optimization resulted in a local minimum structure, we carried out a complete normal-mode analysis for the most stable structures of the complexes H_mRh_n/ZO (m = 1, 3, 5, 7 for n = 3 and m = 1, 3, 5, 7, 9 for n = 4), including all degrees of freedom of the complex and the zeolite framework. No imaginary vibrational frequency was found. The vibrational frequencies were calculated in the harmonic approximation by diagonalizing the mass-weighted Hessian matrix. The matrix was constructed from finite differences of the first-order derivatives of the total energy, by shifting each of the ions from the optimized structure in all Cartesian directions.

The atomic charges of the complexes H_mRh_n/ZO were calculated using a Bader-type analysis.[24]

We evaluated the stability of the species by relative energies, ΔE, and various types of binding energies, BE, defined as follows:

—relative stability ΔE with respect to the most stable structure of the same composition,

—binding energy (BE) of the Rh_n cluster (n = 3, 4) to the zeolite framework leading to formation of bare Rh_n/ZOH or hydrogenated HRh_n/ZO species:

$$\mathrm{BE}(\mathrm{Rh}_n) = E(\mathrm{Rh}_n/\mathrm{ZOH}) - E(\mathrm{ZOH}) - E(\mathrm{Rh}_n)$$

$$\mathrm{BE}(\mathrm{HRh}_n) = E(\mathrm{HRh}_n/\mathrm{ZO}) - E(\mathrm{ZOH}) - E(\mathrm{Rh}_n)$$

—average BE of H atoms on the cluster HRh_n adsorbed in a zeolite cage with respect to H_2 in the gas phase:

$$\mathrm{BE}_{\mathrm{av}}(\mathrm{H}) = [E(\mathrm{H}_m\mathrm{Rh}_n/\mathrm{ZO}) - E(\mathrm{HRh}_n/\mathrm{ZO})]/(m-1) - E(\mathrm{H}_2)/2$$

DOI: 10.1021/jp510842q
J. Phys. Chem. C 2015, 119, 1121−1129

—average BE per H atom from adding the last H_2 molecule to the supported cluster $H_{m-2}Rh_n/ZO$:

$$BE_l(H) = [E(H_mRh_n/ZO) - E(H_{m-2}Rh_n/ZO)]/2 - E(H_2)/2$$

Note that all BE values are calculated with respect to the most stable structure of the corresponding composition.

2.3. Thermodynamic Models. Using the relative Gibbs free energies of the H_mRh_n/ZO systems under study, we constructed a thermodynamic model for the hydrogen coverage of the rhodium clusters as a function of the temperature and the H_2 pressure. The relative Gibbs free energy, $\Delta G(H_mRh_n/ZO)$, of a structure H_mRh_n/ZO (n = 3, 4) is defined via its formal formation from the corresponding bare metal species Rh_n, supported in the zeolite, after adsorption of $m/2H_2$ molecules from the gas phase

$$Rh_n/ZO + m/2H_2 \rightarrow H_mRh_n/ZO$$

$$\Delta G(H_mRh_n/ZO) = \Delta H(H_mRh_n/ZO) - T\Delta S(H_mRh_n/ZO)$$

Here $\Delta H(H_mRh_n/ZO)$ is the corresponding change in enthalpy (including the electronic energy and the zero-point energy correction), and $\Delta S(H_mRh_n/ZO)$ is the change in entropy, determined in standard fashion from the partition functions q of the corresponding clusters and the appropriate number of H_2 molecules, for systems in the gas phase.[25] The free rotation and the free translation were taken into account only for the H_2 molecules but not for the systems H_mRh_n/ZO.

The equilibrium constant, $K(H_mRh_n/ZO)$, for formally forming the complex H_mRh_n/ZO from the corresponding supported bare cluster Rh_n/ZO and the appropriate amount of H_2 molecules can be obtained from the Gibbs free energy of the reaction, on the one hand, and, on the other hand, can be presented in terms of mole fractions, α_m, of the adsorption complexes containing m hydrogen ligands and the hydrogen pressure, $P(H_2)$, in the gas phase[25,26]

$$K(H_mRh_n/ZO) = \exp[-\Delta G(H_mRh_n/ZO)/RT] = [\alpha_m(RT)^{m/2}]/[\alpha_0 P^{m/2}(H_2)]$$

To define the molar fractions for complexes with various amounts of hydrogen, we use the following expressions

$$\alpha_0 = \{1 + \sum_{m_{odd}}^{m_{max}} [[P(H_2)/RT]^{m/2} K(H_mRh_n/ZO)]\}^{-1}$$

$$\alpha_m = \alpha_0 [P(H_2)/RT]^{m/2} K(H_mRh_n/ZO)$$

Here m_{max} is 9 for Rh_4 and 7 for Rh_3 species. Note that these expressions consider only the species with odd values of m and the supported bare cluster Rh_n/ZO, which corresponds to interpolating the Gibbs free energy values for the species with even value of m, similar to the approach that we reported earlier for hydrogenated iridium clusters in a zeolite.[26]

3. RESULTS

We started our investigation by optimizing the bare Rh_n clusters (n = 3, 4) supported on the zeolite framework. In agreement with previous studies,[10,27,28] our calculations showed that hydrogen spillover of the H atom from the bridging hydroxyl group to the Rh_n clusters is energetically favorable. The most stable complex with a bare Rh_3 cluster, at 6R, is by 217 kJ/mol less stable than the most stable complex HRh_3/ZO (at 4R) after H spillover; for details, see Table S1 in the SI. The structures with bare Rh_4 clusters are also significantly less stable than the complexes HRh_4/ZO after reverse H spillover from the bridging OH group. The most stable bare metal complex Rh_4/ZOH (at 6R) is by 177 kJ/mol less stable than the most stable hydrogenated cluster HRh_4/ZO (at 4R); see Table S5 of the SI. Therefore, in the following we will refrain from discussing bare supported Rh_n clusters.

3.1. Structural Properties of Hydrogenated Rhodium Clusters. We will address three structural features of hydrogenated complexes: (i) the location of the clusters at the zeolite framework; (ii) changes of the shape of the metal moieties due to hydrogen loading; and (iii) the location of the H ligands on the clusters. We will start with the complexes formed after reverse H spillover, HRh_3/ZO and HRh_4/ZO, and will continue with complexes formed after adsorption of hydrogen from the gas phase, H_mRh_3/ZO and H_mRh_4/ZO. The optimized geometries of the most stable structures obtained with Rh_3 and Rh_4 clusters near 4R and 6R are shown in Figure 2. Tables 1 and 2 present selected structural parameters of H_mRh_3/ZO and H_mRh_4/ZO systems, respectively, their relative stability, and calculated adsorption energies of hydrogen.

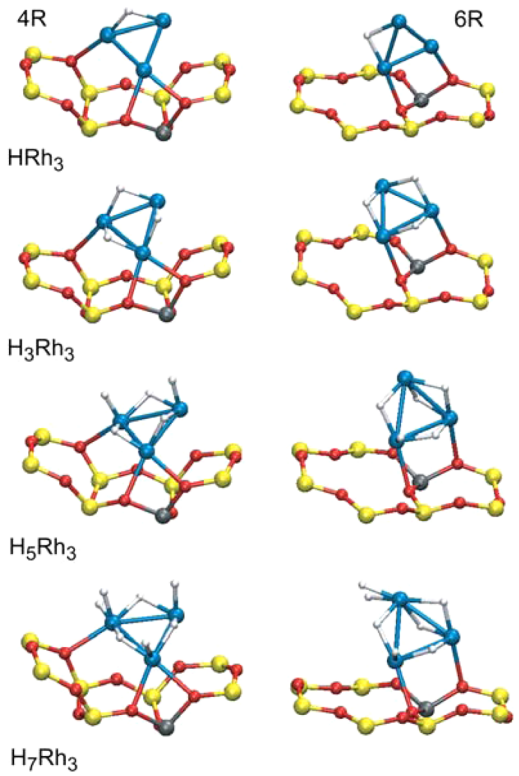

Figure 2. Sketches of optimized structures of the most stable complexes H_mRh_3/ZO with different hydrogen loading, at 4R sites (left-hand column) and 6R sites (right-hand column).

3.1.1. Location of the Metal Clusters. The coordination of the metal clusters near the 4R site is similar for both HRh_3 and HRh_4. One Rh atom interacts with two O centers in the immediate vicinity of the Al center of the ring (Figure 1). In the two series of hydrogenated complexes the Rh−O distances are in the typical range, 222−231 pm for H_mRh_3/ZO and 215−235

DOI: 10.1021/jp510842q
J. Phys. Chem. C 2015, 119, 1121−1129

Table 1. Energetic (kJ/mol) and Structural (pm) Characteristics of Complexes with Rh_3 Clusters after Adsorption Of H Atoms

complex	n_{Ht}, n_{Hbr} [a]	Ns[b]	⟨Rh−Rh⟩[c]	Rh−O, n[d]	ΔE[e]	$BE_{av}(H)$[f]	$BE_1(H)$[g]
HRh_3/ZO-4R	0, 1	3	242	227, 3	0		
HRh_3/ZO-6R	0, 1	3	242	221, 2	29		
H_3Rh_3/ZO-4R	0, 3	1	250	225, 3	0	−70	−70
H_3Rh_3/ZO-6R	0, 3	3	254	226, 2	44	−47	−47
H_5Rh_3/ZO-4R	2, 3	1	260	230, 3	0	−61	−52
H_5Rh_3/ZO-6R	1, 4	1	265	227, 2	33	−53	−36
H_7Rh_3/ZO-4R	4, 3	1	272	231, 3	1	−52	−36
H_7Rh_3/ZO-6R	3, 4	1	268	227, 2	0	−51	−36

[a]Number of terminal and bridge coordinated ligands on the cluster Rh_3. [b]Number of unpaired electrons in the system. [c]Average Rh−Rh distance. [d]Average value of the short Rh−O distances, number n of such contacts. [e]Relative stability. [f]Average binding energy of the H atom on the cluster HRh_3 adsorbed in the zeolite. [g]Binding energy per H atom of the two H ligands last added to the cluster. For definitions of the energy values see Section 2.

Table 2. Energetic (kJ/mol) and Structural (pm) Characteristics of Complexes with Rh_4 Clusters after Adsorption of H Atoms

complex	n_{Ht}, n_{Hbr} [a]	Ns[b]	⟨Rh−Rh⟩[c]	Rh−O, n[d]	ΔE[e]	$BE_{av}(H)$[f]	$BE_1(H)$[g]
HRh_4/ZO-4R	0, 1	0	247	230, 3	0		
HRh_4/ZO-6R	0, 1	0	247	226, 2	14		
H_3Rh_4/ZO-4R	0, 3	2	255	228, 3	0	−67	−67
H_3Rh_4/ZO-6R	0, 3	0	256	224, 3	22	−56	−56
H_5Rh_4/ZO-4R	2, 3	0	256	230, 4	0	−55	−42
H_5Rh_4/ZO-6R	2, 3	0	260	224, 2	55	−41	−26
H_7Rh_4/ZO-4R	4, 3	0	261	226, 3	0	−50	−40
H_7Rh_4/ZO-6R	4, 3	0	274	227, 2	42	−43	−19
H_9Rh_4/ZO-4R	5, 4	0	265	226, 3	0	−47	−40
H_9Rh_4/ZO-6R	4, 5	0	269	226, 3	1	−47	−40

[a]Number of terminal and bridge coordinated ligands on the cluster Rh_4. [b]Number of unpaired electrons in the system. [c]Average Rh−Rh distance. [d]Average value of the short Rh−O distances, number n of such contacts. [e]Relative stability. [f]Average binding energy of the H atom on the cluster HRh_4 adsorbed in the zeolite. [g]Binding energy per H atom of the two H ligands last added to the cluster. For definitions of the energy values see Section 2.

pm for H_mRh_4/ZO (Tables 1 and 2). These distances slowly decrease with hydrogen loading, correlating as a general trend with the increasing positive charge on the metal moiety; see Section 3.5 and the SI (Tables S9 and S10). In the structures with high coverage (more than 5 H ligands), one of the Rh−O distances is around 215 pm, in good agreement with the distance estimated from EXAFS measurements, 217 pm.[29] The adjacent Rh atom in the cluster is coordinated to another O atom from a neighboring four-membered ring, at longer Rh−O distances, 230−237 pm, for various H loadings. Rh−Al distances are calculated in the ranges 281−291 pm for H_mRh_3/ZO complexes and 290−295 pm for H_mRh_3/ZO complexes.

Different types of coordination are determined for the hydrogenated rhodium clusters that are located near a 6R site. Two Rh atoms of the H_mRh_3/ZO complexes are coordinated to different oxygen atoms that are directly bonded to the Al center. One of the oxygen atoms is part of the six-membered ring, and the second one is from a neighboring four-membered ring (Figures 1 and 2). The Rh−O distances fall into the range 220−229 pm (Tables 1 and 2). The H_mRh_4/ZO complexes are located above the plane of the 6R site, close to the Al center. Two Rh−O contacts occur between two Rh atoms at the bottom of the Rh_4 tetrahedron, each interacting with a separate O atom of the 6R site. These Rh atoms are coordinated to O centers directly connected to the Al center. The shortest Rh−O distance slowly decreases with hydrogen loading, from 224 to 215 pm, approaching the experimental value, 217 pm.[29] The third short Rh−O distance, to an O center from a Si−O−Si bridge, is ∼230 pm. This coordination is modified for the complex H_9Rh_4/ZO at 6R, where one of the Rh centers is interacting with two O atoms of the 6R site, with Rh−O = 224, 240 pm. The Rh−Al distances are calculated longer than those for clusters located at the 4R site, 286−308 pm for H_mRh_3/ZO complexes and 324−330 pm for H_mRh_4/ZO complexes.

For hydrogenated clusters containing four or six rhodium atoms as well as for Rh^+ species, average Rh−O distances of 216−218 pm were calculated earlier using isolated or embedded zeolite fragments.[9,10,14,18]

3.1.2. Structural Changes in the Shape of the Metal Clusters. The average Rh−Rh distances in the HRh_n/ZO species formed after hydrogen spillover from the bridging OH group remain the same as those calculated for the clusters in the gas phase, 242 pm for Rh_3 and 247 pm for Rh_4 (Tables 1 and 2). Figure 3 shows the change of the average intermetal distances ⟨Rh−Rh⟩ with H loading of the metal moieties. In the complexes H_mRh_3/ZO ⟨Rh−Rh⟩ increases almost linearly with H loading, from 242 pm for HRh_3/ZO to 272 pm for H_7Rh_3/ZO.

In the complexes H_mRh_4/ZO located near 4R, ⟨Rh−Rh⟩ values are calculated shorter than in the analogous complexes near 6R. With increasing number of H ligands, the lengths of the individual Rh−Rh bonds scatter more; see Tables S11 and S12 in the SI. In the complex H_7Rh_4/ZO located near a six-membered ring (6R), one of the Rh−Rh bonds, 343 pm, is essentially broken, and the shape of the metal moiety is no longer a (distorted) tetrahedron (Figure 3). Addition of the last two H atoms to this structure results in a reorientation of the cluster, and its tetrahedral shape is restored.

DOI: 10.1021/jp510842q
J. Phys. Chem. C 2015, 119, 1121−1129

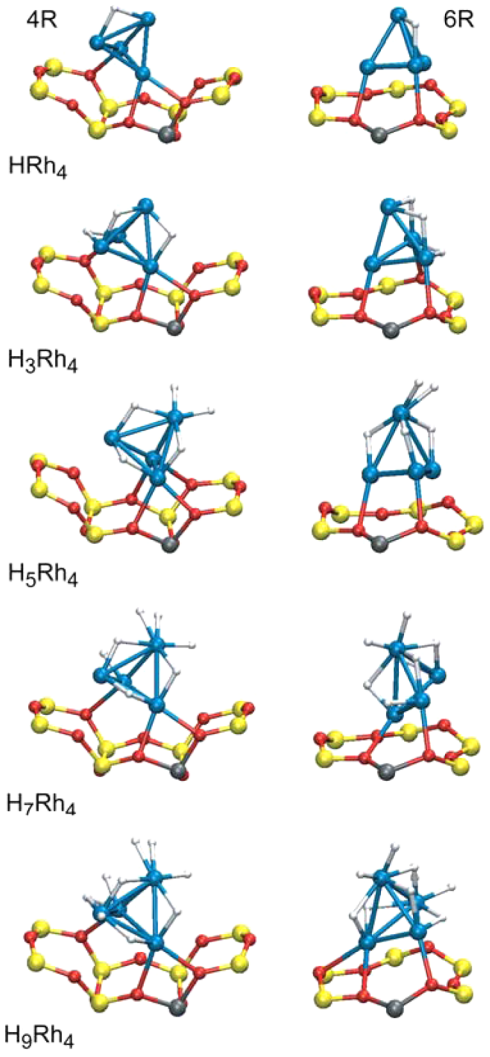

Figure 3. Sketches of optimized structures of the most stable complexes H_mRh_4/ZO with different hydrogen loading, at 4R sites (left-hand column) and 6R sites (right-hand column).

In general, H loading of the complexes H_mRh_n/ZO leads to an increase of ⟨Rh−Rh⟩ (Figure 4). Previous studies on Ir_4, Rh_6, and Rh_4 clusters,[9] supported on isolated zeolite fragments, reported an elongation of the average metal−metal distances upon hydrogenation. In the present models, the larger ⟨Rh−Rh⟩ values are mainly due to elongated Rh−Rh bonds at which bridging H ligands are coordinated. Such Rh−Rh bonds are elongated by 2−20 pm; see Tables S11 and S12 in the SI. ⟨Rh−Rh⟩ values of structures with high H loading, five and more H atoms adsorbed, are in the range 260−274 pm (Figure 4), close to the experimentally determined value of 270 pm.[29]

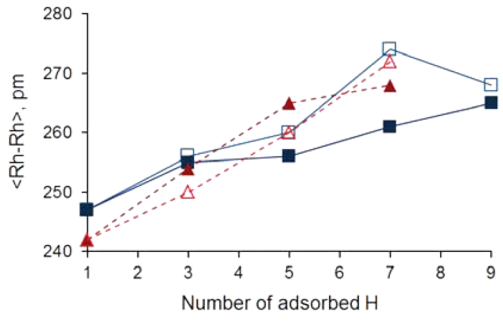

Figure 4. Calculated average Rh−Rh distances in the complexes H_mRh_3/ZO (dashed red line) and H_mRh_4/ZO (solid blue line) vs the number of hydrogen ligands on the metal cluster. Filled symbols correspond to complexes located at 4R sites and empty symbols to complexes located at 6R sites.

3.1.3. Location of the H Ligands. We determined two types of stable adsorption modes of H ligands at the metal moiety, at bridge and terminal positions. Rh−H distances are longer for bridging coordination, 162−195 pm. In contrast, Rh−H distances for terminal coordination are shorter, in the range 154−161 pm; see Tables S13 and S14 in the SI. These results agree well with those of previous calculations for clusters on isolated zeolite fragments.[9,10] In addition to the ligands with H−H distances larger than 180 pm, which are considered as dissociated, some of the ligands in the present complexes with high H loading are coordinated to the cluster in the form of activated hydrogen molecules, with H−H distances in the range 88−93 pm. In these cases, the Rh−H distances are longer, 166−174 pm, than for H ligands in terminal coordination.

An earlier computational study on isolated zeolite fragments as models reported comparable Rh−H distances for ligands in bridge positions, 157−204 pm, and at terminal sites, 155−156 pm.[9]

3.2. Stability of Hydrogenated Rhodium Clusters.

3.2.1. Relative Stability. The relative stability, ΔE, of the complexes studied will be discussed in relation to the location of the complex at the zeolite framework and the preferable coordination of the hydrogen ligands. As described in Section 2, ΔE is determined with respect to the most stable structure of the same composition. The calculated values for the most stable structures at 4R and 6R sites are reported in Tables 1 and 2, and those for all modeled structures are shown in Tables S1, S3, S5, and S7 of SI.

***Rh*$_3$.** For the structures with one to five H ligands, the complexes H_mRh_3/ZO are preferentially located at 4R sites. The relative stability, ΔE, of the corresponding structures at the 6R site varies with hydrogen loading: 29 kJ/mol with 1 H ligand, 44 kJ/mol with 3 H, and 33 kJ/mol with 5 H (Table 1). The complexes with highest hydrogen loading, H_7Rh_3/ZO, are essentially equally stable at the 4R and the 6R sites.

The hydrogen transferred from the bridging OH group to the rhodium cluster prefers to coordinate in 2-fold fashion, irrespective of the location of the cluster and the initial position of the ligand. No structures with terminal ligands were found because the H ligand moves to the bridge position during the optimization. The bridge coordination of H ligands is favored until all three Rh−Rh bonds are bridged by a ligand. In the structures with more than three adsorbed hydrogen atoms, the additional ligands prefer terminal binding.

***Rh*$_4$.** Similarly to the hydrogenated Rh_3 cluster, the H_mRh_4/ZO species prefer the location at a 4R site. The structures at the 6R site are by 14 kJ/mol for 1 H ligand, 22 kJ/mol for 3 H, 55 kJ/mol for 5 H, and 42 kJ/mol for 7 H less stable than the same species at the 4R sites (Table 2). Note that the largest difference in stability between the two locations is determined for the structures H_5Rh_4/ZO. The most stable structures of the complexes formed after adsorption of eight H ligands, H_9Rh_4/ZO, have essentially the same stability at 4R and at 6R sites, just as obtained for the H_mRh_3/ZO species. The higher stability of this particular structure at the 6R site may be due to an additional short Rh−O contact (Figure 3, Table 2), as one Rh atom is coordinated to two oxygen centers of the six-membered

DOI: 10.1021/jp510842q
J. Phys. Chem. C 2015, 119, 1121−1129

ring. This coordination goes along with the regeneration of the tetrahedral shape of the metal moiety and a somewhat shorter ⟨Rh−Rh⟩ value, 268 pm, compared to 274 pm for the H_7Rh_4/ZO complex at the same site.

The most stable complexes HRh_4/ZO, formed after reverse H spillover from the bridging OH group, have the H ligand in bridge coordination for both 4R and 6R sites. The structures with terminal coordination of the (first) H ligand are by 102 kJ/mol (4R) and 132 kJ/mol (6R) less stable (Table S5 of the SI). In the complexes with two more H ligands, H_3Rh_4/ZO, the bridge coordination of the ligands remains more stable, and in the most stable structures all three ligands are at Rh−Rh bridge sites. The most stable H_5Rh_4/ZO complexes have three bridge and two terminal H ligands, while the optimized structures with more than three bridging ligands are less stable by 43 kJ/mol. For hydrogen coverages from 3 to 7 H ligands, the most stable structures have three bridge coordinated ligands; more bridging H ligands results in less stable systems. Only the complexes with the highest hydrogen loading modeled, H_9Rh_4/ZO, have four bridging and five terminal or five bridging and four terminal ligands at 4R and 6R sites, respectively (Table 2).

3.2.2. Adsorption Energy of Hydrogen. The affinity of zeolite-supported rhodium clusters toward hydrogen adsorption is well documented.[9,10] It may be estimated by the average binding energy, $BE_{av}(H)$, of H ligands of the complexes H_mRh_n/ZO and the binding energy, $BE_l(H)$, added last to the corresponding complex $H_{m-2}Rh_n$/ZO. Both energy values are calculated per H atom (Section 2.2) and are reported in Tables 1 and 2; see also Figure 5.

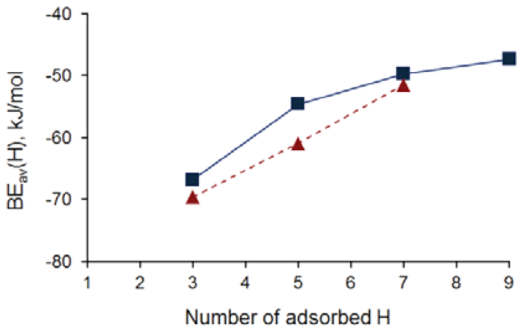

Figure 5. Calculated average binding energies of hydrogen atoms, $BE_{av}(H)$, in the most stable complexes H_mRh_3/ZO (dashed red line) and H_mRh_4/ZO (solid blue line) vs the number of hydrogen ligands on the metal cluster.

***Rh*$_3$.** For the Rh_3-type clusters, the $BE_{av}(H)$ value of the first two hydrogen ligands in the most stable complex H_3Rh_3/ZO, located at the 4R site, is −70 kJ/mol per H atom. The adsorption energy decreases (in absolute terms) to −61 kJ/mol for the most stable structure with 5 H ligands and further to −51 kJ/mol in the complex with 7 H ligands. The BE_l values exhibit the essentially same trend; this quantity decreases from −70 kJ/mol for the first two H ligands atoms to −36 kJ/mol for the complex H_7Rh_3/ZO at the 4R site. The BE_l values for complexes at the 6R site indicate a slightly less strong interaction. They vary from −47 kJ/mol for the complex H_3Rh_3/ZO to −36 kJ/mol for the analogous Rh_3-type complexes with five and seven ligands.

***Rh*$_4$.** We determined similar results for the adsorption complexes with Rh_4-type clusters. The average adsorption energy of hydrogen, $BE_{av}(H)$, on the HRh_4/ZO complex decreases with hydrogen loading (Figure 5). The value for the complex H_3Rh_4/ZO at a 4R site is −67 kJ/mol per H ligand, which agrees well with the value, −72 kJ/mol, calculated earlier for the cluster H_3Rh_4 supported on a finite zeolite model.[9] The $BE_{av}(H)$ values for the complexes with 5, 7, and 9 H ligands decrease (in absolute value) to −55, −50, and −47 kJ/mol, respectively (Table 2, Figure 5). The calculated binding energies $BE_l(H)$ for structures with 5−9 H ligands change slightly for the complexes located at 4R sites, from −42 to −40 kJ/mol. The corresponding values for the complexes near 6R sites vary more, from −19 to −40 kJ/mol. The former value corresponds to the structure with 7 H ligands, and the latter value was obtained for the complex with nine ligands. The $BE_l(H)$ value of the complex H_9Rh_4/ZO at a 6R site after addition of the last two H ligands was higher (in absolute value) than the analogous results for less H loading, and we generated additional initial structures of the complexes H_5Rh_4/ZO and H_7Rh_4/ZO. However, after geometry optimization the stability of those complexes was lower than the original structures at 6R sites with the same number of H ligands.

The values calculated for the average binding energies of H on the supported clusters Rh_3 and Rh_4 are very similar. For the most stable structures at the site 4R, the values of Rh_3 complexes are slightly larger, at most by 6 kJ/mol (Figure 5).

Figure 5 shows a clear trend to lower absolute values of the binding energy of hydrogen for increasing hydrogen loading, calculated earlier for zeolite-supported Rh_4 clusters supported on isolated fragments.[9] The binding energies decrease from −72 kJ/mol (H_3Rh_4) to −38 kJ/mol (H_9Rh_4). Analogous trends, but with lower slopes, were calculated for other M_4 clusters on zeolite fragments and the same range of hydrogen loadings: −72 to −52 kJ/mol for Ir_4 and from −62 to −52 kJ/mol for Pt_4.[9]

3.3. Thermodynamic Model for Hydrogen Adsorption on Rhodium Clusters. The thermodynamic models, derived from calculated free energies, allowed us to determine the stable hydrogenated species for given temperature and pressure conditions. The phase diagrams in Figure 6 show the dominant type of complex according to the calculated molar fractions (see Section 2.3). The lines correspond to equal molar fractions of the complexes in the two neighboring areas. According to these phase diagrams, strongly dehydrogenated species for both types of rhodium clusters, HRh_3/ZO and HRh_4/ZO, can be expected at temperature above 450 K and at a hydrogen pressure below 10 Pa. Fully dehydrogenated zeolite-supported Rh_4 species may be stabilized only at very high temperature, at 800 K and above, and hydrogen pressure below 10^{-5} Pa. Complexes with intermediate H loading, H_mRh_3/ZO (m = 3, 5) and H_mRh_4/ZO (m = 3, 5, 7), can preferably be found only in a relatively narrow region of temperature and H_2 pressure (Figure 6). In contrast, complexes with highest hydrogen loading modeled, H_7Rh_3/ZO and H_9Rh_4/ZO, are preferable in wide ranges of temperature and hydrogen pressure. These complexes dominate at about 300 K even for the lowest considered pressure (10^{-5} Pa) as well as at temperatures above 700 K when $P(H_2)$ is higher than 10^4 Pa. As described above, the addition of the last two H ligands to each of the modeled clusters results in formation of an activated H_2 molecule, which suggests that it is unlikely to have (notably) more ligands on the cluster than those modeled here.

The experimental conditions under which zeolite-supported rhodium clusters have been examined experimentally vary with the pretreatment and the catalytic procedure. For example, the

DOI: 10.1021/jp510842q
J. Phys. Chem. C 2015, 119, 1121−1129

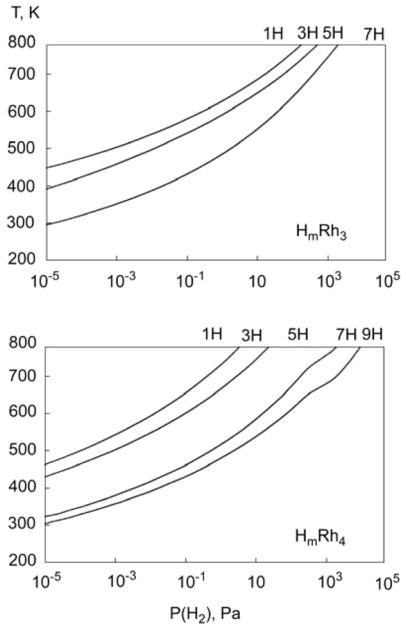

Figure 6. Phase diagram as a function of temperature T and hydrogen pressure $P(H_2)$, indicating regions where the complexes H_mRh_3/ZO (upper panel) and H_mRh_4/ZO (lower panel) with m H ligands dominate. The regions specified correspond to species with concentrations above 50%.

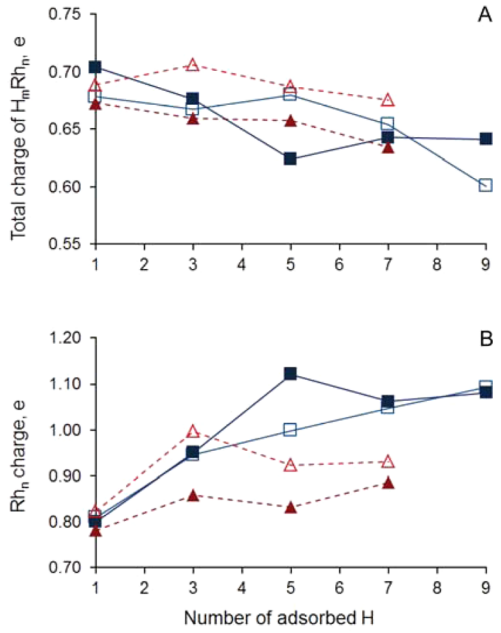

Figure 7. Calculated Bader charges of $[H_mRh_n]$ complexes including the metal cluster and the H ligands (A) and of the Rh_n moiety (B) in the complexes H_mRh_3/ZO (dashed red line) and H_mRh_4/ZO (solid blue line). Filled and empty symbols correspond to complexes located at 4R and 6R sites, respectively.

Rh/zeolite samples during ethene hydrogenation have in part been treated at 298 K and H_2 pressure near 10^5 Pa.[29] Thus, maximum hydrogen loading of the rhodium clusters is expected according to the present modeling. Indeed, the measured Rh−Rh distance under such conditions, 269−270 pm, fits quite well the average Rh−Rh distance calculated for the most stable clusters with three and four metal atoms, 268 and 265 pm (Figure 4). Also the pretreatment conditions, 473 K and $P(H_2)$ = 10^5 Pa, of other rhodium-containing catalytic samples,[30] correspond to the formation of clusters with maximum hydrogen loading.

3.4. Charges of Hydrogenated Rhodium Clusters. The charge distributions of the adsorbed complexes were determined to analyze the electronic characteristics of small zeolite-supported Rh clusters under H loading. Figure 7A shows the change in the total charge of the rhodium moiety in the H_mRh_n/ZO clusters with hydrogen loading at the two sites, 4R and 6R. The calculated positive charge of the Rh_3 moiety in the H_mRh_3/ZO complexes varies from 0.78 to 1.00 e (Figure 7B). Increasing the H loading of the complex leads to a small decrease of the total positive charge of the moiety $[H_mRh_3]$, from 0.70 to 0.64 e.

The charge calculated for the Rh_4 moiety of the complexes H_mRh_4/ZO at site 6R increases almost linearly with the hydrogen loading, from 0.80 to 1.09 e (Figure 7B). In contrast, the trend for the complexes at site 4R is not monotonic; the corresponding values vary from 0.80 to 1.12 e. Similar to our earlier calculations on zeolite-supported transition metal clusters,[13] rhodium centers directly coordinated to oxygen centers of the zeolite framework are oxidized and have higher charges, ∼0.35 e, than other Rh centers in the clusters (Tables S9 and S10 of SI). The presence of hydrogen ligands directly bonded to a Rh atom results in a decrease of its positive charge. The Rh_4 moiety of the complex H_5Rh_4/ZO at site 4R has the highest calculated positive charge, 1.12 e (Figure 7B). In this system, the Rh atom interacting with two O centers from the zeolite framework has a positive charge of 0.47 e. On the other hand, the total charge of the $[H_mRh_4]$ complexes decreases slightly with increasing H loading, from 0.70 to 0.60 e, due to the small negative charge of the hydrogen ligands, ranging from −0.01 to −0.12 e.

These variations agree with results of our earlier studies on hydrogenated transition metal clusters.[9,12] Previously we noted that the main contribution to the oxidation of the supported metal moieties M_n is due to reverse H spillover. In the present work, this mechanism accounts for 0.8 e of the positive charge of the complexes HRh_3/ZO and HRh_4/ZO.[9] As already shown for the Ir_4 cluster,[12] when the metal cluster has charge 0 or 1 e, as in the present case for the complexes HRh_3/ZO and HRh_4/ZO, adsorption of additional hydrogen results in a partial oxidation of the metal moiety. However, this additional oxidation contributes only ∼0.1 e for Rh_3 complexes and 0.3 e for Rh_4 complexes.

4. CONCLUSIONS

We have studied computationally the adsorption of hydrogen on small rhodium clusters Rh_3 and Rh_4 that are supported in a faujasite-type zeolite. To account accurately for the role of the zeolite framework, we used periodic density functional calculations. We modeled two preferential sites of the metal clusters in the supercavity of faujasite, near a six-membered ring (6R) and near three four-membered rings (4R), and we explored the coordination of the H ligands depending on the hydrogen loading.

Three Rh−O contacts were determined for the coordination near site 4R, and two of them involve framework oxygen centers that are directly bonded to the Al center of the zeolite. For coordination near 6R in most cases only two short Rh−O distances are present, again with the O atoms bonded to the Al center. Concomitant with hydrogen loading, positive charges

DOI: 10.1021/jp510842q
J. Phys. Chem. C 2015, 119, 1121−1129

on the metal moieties increase, and Rh−O distances decrease, reaching values close to the experimental value, 217 pm, determined by EXAFS. Average Rh−Rh distances increase with hydrogen loading, mainly due to H ligands in bridge coordination. The ⟨Rh−Rh⟩ values increase from 242 to 272 pm for Rh_3 complexes and from 247 to 265 pm for complexes for Rh_4 complexes. The ⟨Rh−Rh⟩ values of species with high hydrogen coverage (more than five H ligands) reach the value found by EXAFS experiments. Bridge coordination of the ligands is favorable for up to four H ligands. Additional H atoms prefer to coordinate in the terminal position. The Rh−H distances are longer for bridge ligands ranging from 162 to 195 pm. For terminal ligands this interval is 154−161 pm.

For all hydrogen loadings, clusters at sites 4R are energetically more stable. The complexes with the highest H loading, H_7Rh_3/ZO and H_9Rh_4/ZO, are equally stable at 4R and 6R sites.

A thermodynamic model based on calculated Gibbs free energies of the structures studied predicts that strongly dehydrogenated species for both types of rhodium clusters (with only 1 H ligand) can be expected at temperature above 450 K and hydrogen pressure below 10 Pa. Structures with intermediate amounts of H ligands adsorbed on the Rh_n clusters are preferred in a relatively narrow range of temperature and H_2 pressure, while the complexes with maximum amounts of ligands, H_7Rh_3/ZO and H_9Rh_4/ZO, dominate in large intervals of temperature and H_2 pressure, probably due to saturation of the metal moieties with hydrogen loading.

■ ASSOCIATED CONTENT

Supporting Information

Tables S1 to S18 present information on the relative stability and the structural parameters of all isomeric structures examined, calculated Bader charges, and Rh−Rh and Rh−H vibrational frequencies of the most stable complexes. Figures showing the location of the metal cluster in the zeolite cavity, the optimized structures of bare supported clusters, Rh_3/ZOH and Rh_4/ZOH, and of hydrogenated clusters supported in FAU at 4R and 6R sites. Cartesian coordinates of the most stable complexes for each hydrogen loading at 4R and 6R sites. This material is available free of charge via the Internet at http://pubs.acs.org.

■ AUTHOR INFORMATION

Corresponding Author

*E-mail: roesch@mytum.de. Phone: +49 89 289 13619.

Notes

The authors declare no competing financial interest.

■ ACKNOWLEDGMENTS

We thank Dr. Alexander Genest and Dr. Petko Petkov for helpful discussions. VKM and GNV gratefully acknowledge funding by the FP7 project Beyond Everest. NR acknowledges a generous grant of computing resources by the Gauss Centre for Supercomputing (www.gauss-centre.eu), provided on the SuperMUC platform of Leibniz Supercomputing Centre Garching (www.lrz.de).

■ REFERENCES

(1) Sachtler, W. M. H.; Zhang, Z. Zeolite-Supported Transition Metal Catalysts. *Adv. Catal.* **1993**, *39*, 129−220.

(2) Hayek, K.; Goller, H.; Penner, S.; Rupprechter, G.; Zimmermann, C. Regular Alumina-Supported Nanoparticles of Iridium, Rhodium and Platinum under Hydrogen Reduction: Structure, Morphology and Activity in the Neopentane conversion. *Catal. Lett.* **2004**, *92*, 1−9.

(3) Vajda, S.; Pellin, M. J.; Greeley, J. P.; Marshall, C. L.; Curtiss, L. A.; Ballentine, G. A.; Elam, J. W.; Catillon-Mucherie, S.; Redfern, P. C.; Mehmood, F.; et al. Subnanometre Platinum Clusters as Highly Active and Selective Catalysts for the Oxidative Dehydrogenation of Propane. *Nat. Mater.* **2009**, *8*, 213−216.

(4) Serna, P.; Gates, B. C. Zeolite- and MgO-supported Rhodium Complexes and Rhodium Clusters: Tuning Catalytic Properties to Control Carbon-Carbon vs. Carbon-Hydrogen Bond Formation Reactions of Ethene in the Presence of H_2. *J. Catal.* **2013**, *308*, 201−212.

(5) Guzman, J.; Gates, B. C. Supported Molecular Catalysts: Metal Complexes and Clusters on Oxides and Zeolites. *Dalton Trans.* **2003**, 3303−3318.

(6) Beneke, M.; Jaeger, N. I.; Schulz-Ekloff, G. In *Host-Guest-Systems Based on Nanoporous Crystals*; Laeri, F., Schüth, F., Simon, U., Wark, M., Eds.; Wiley-VCH: Weinheim, 2003; pp 165−182.

(7) Oudenhuijzen, M. K.; van Bokhoven, J. A.; Ramaker, D. E.; Koningsberger, D. C. Theoretical Study on Pt Particle Adsorbate Bonding: Influence of Support Ionicity and Implications for Catalysis. *J. Phys. Chem. B* **2004**, *108*, 20247−20254.

(8) Kip, B. J.; Duivenvoorden, F. B. M.; Koningsberger, D. C.; Prins, R. Determination of Metal Particle Size of Highly Dispersed Rh, Ir, and Pt Catalysts by Hydrogen Chemisorption and EXAFS. *J. Catal.* **1987**, *105*, 26−38.

(9) Petkov, P., St.; Petrova, G. P.; Vayssilov, G. N.; Rösch, N. Saturation of Small Supported Metal Clusters by Adsorbed Hydrogen. A Computational Study on Tetrahedral Models of Rh_4, Ir_4, and Pt_4. *J. Phys. Chem. C* **2010**, *114*, 8500−8506.

(10) Vayssilov, G. N.; Petrova, G. P.; Ivanova Shor, E. A.; Nasluzov, V. A.; Shor, A. M.; Petkov, P., St.; Rösch, N. Reverse Hydrogen Spillover on and Hydrogenation of Supported Metal Clusters: Insights from Computational Model Studies. *Phys. Chem. Chem. Phys.* **2012**, *14*, 5879−5890.

(11) Petrova, G. P.; Vayssilov, G. N.; Rösch, N. Density Functional Modeling of Reverse Hydrogen Spillover on Zeolite-Supported Tetrairidum Clusters. *Chem. Phys. Lett.* **2007**, *444*, 215−219.

(12) Petrova, G. P.; Vayssilov, G. N.; Rösch, N. Redox Behavior of Small Metal Clusters with Respect to Hydrogen. The Effect of the Cluster Charge from Density Functional Results. *Phys. Chem. Chem. Phys.* **2010**, *12*, 11015−11020.

(13) Ivanova Shor, E. A.; Nasluzov, V. A.; Shor, A. M.; Vayssilov, G. N.; Rösch, N. Reverse Hydrogen Spillover onto Zeolite-Supported Metal Clusters: An Embedded Cluster Density Functional Study of Models M6 (M = Rh, Ir, Au). *J. Phys. Chem. C* **2007**, *111*, 12340−12351.

(14) Shor, A. M.; Ivanova Shor, E. A.; Laletina, S.; Nasluzov, V. A.; Vayssilov, G. N.; Rösch, N. Effect of the Size of the Quantum Region in a Hybrid Embedded-cluster Scheme for Zeolite Systems. *Chem. Phys.* **2009**, *363*, 33−41.

(15) Baerlocher, C.; McCusker, L. B.; Olson, D. H. *Atlas of Zeolite Framework Types*, 7th ed.; Elsevier, New York, 2007; http://www.iza-structure.org/databases.

(16) Dinda, S.; Govindasamy, A.; Genest, A.; Rösch, N. Modeling Catalytic Steps on Extra-Framework Metal Centers in Zeolites. A Case Study on Ethylene Dimerization. *J. Phys. Chem. C* **2014**, *118*, 25077−25088.

(17) Sierka, M.; Eichler, U.; Datka, J.; Sauer, J. Heterogeneity of Brønsted Acidic Sites in Faujasite Type Zeolites Due to Aluminum Content and Framework Structure. *J. Phys. Chem. B* **1998**, *102*, 6397−6404.

(18) Ivanova Shor, E. A.; Shor, A. M.; Nasluzov, V. A.; Vayssilov, G. N.; Rösch, N. Effects of the Aluminum Content of a Zeolite Framework: A DFT/MM Hybrid Approach Based on Cluster Models Embedded in an Elastic Polarizable Environment. *J. Chem. Theory Comput.* **2005**, *1*, 459−471.

DOI: 10.1021/jp510842q
J. Phys. Chem. C 2015, 119, 1121−1129

(19) Kresse, G.; Furthmüller, J. Efficiency of Ab-Initio Total Energy Calculations for Metals and Semiconductors Using a Plane-Wave Basis Set. *Comput. Mater. Sci.* **1996**, *6*, 15−50.
(20) Kresse, G.; Furthmüller, J. Efficient Iterative Schemes for Ab-initio Total-energy Calculations Using a Plane-wave Basis Set. *Phys. Rev. B* **1996**, *54*, 11169.
(21) Perdew, J. P.; Burke, K.; Ernzerhof, M. Generalized Gradient Approximation Made Simple. *Phys. Rev. Lett.* **1996**, *77*, 3865.
(22) Blöchl, P. E. Projector Augmented-wave Method. *Phys. Rev. B* **1994**, *50*, 17953.
(23) Kresse, G.; Joubert, D. From Ultrasoft Pseudopotentials to the Projector augmented-wave Method. *Phys. Rev. B* **1999**, *59*, 1758.
(24) Tang, W.; Sanville, E.; Henkelman, G. A Grid-based Bader Analysis Algorithm without Lattice Bias. *J. Phys.: Condens. Matter* **2009**, *21*, 084204−084207.
(25) Atkins, P. W. *Physical Chemistry*, 7th ed.; Oxford University Press: Oxford, 2002.
(26) Petrova, G. P.; Vayssilov, G. N.; Rösch, N. Hydrogen Adsorption on Zeolite-supported Tetrairidium Clusters. Thermodynamic Modeling from Density Functional Calculations. *J. Phys. Chem. C* **2008**, *112*, 18572−18577.
(27) Vayssilov, G. N.; Gates, B. C.; Rösch, N. Oxidation of Supported Rhodium Clusters from Surface Hydroxyl Groups of the Support. *Angew. Chem., Int. Ed.* **2003**, *42*, 1391−1394.
(28) Vayssilov, G. N.; Rösch, N. Free and Zeolite-Supported Hexarhodium Clusters Affected by Adsorbed Light Atoms. *J. Phys. Chem. B* **2004**, *108*, 180−197.
(29) Serna, P.; Gates, B. C. Zeolite-Supported Rhodium Complexes and Clusters: Switching Catalytic Selectivity by Controlling Structures of Essentially Molecular Species. *J. Am. Chem. Soc.* **2011**, *133*, 4714−4717.
(30) Weber, W. A.; Gates, B. C. Rhodium Supported on Faujasites: Effects of Cluster Size and CO Ligands on Catalytic Activity for Toluene Hydrogenation. *J. Catal.* **1998**, *180*, 207−217.

DOI: 10.1021/jp510842q
J. Phys. Chem. C 2015, 119, 1121−1129